# Phase-Shifting Point Diffraction Interferometry for At-Wavelength Testing of Lithographic Optics

E. Tejnil [a, b], K. A. Goldberg [a, c], H. Medecki [a], R. Beguiristain [a, d], J. Bokor [a, b], D. T. Attwood [a, b].

[a] *Center for X-Ray Optics, Lawrence Berkeley National Laboratory, Berkeley, CA 94720*
[b] *Department of Electrical Engineering and Computer Sciences, University of California, Berkeley, CA 94720*
[c] *Department of Physics, University of California, Berkeley, CA 94720*
[d] *Department of Nuclear Engineering, University of California, Berkeley, CA 94720*

## Abstract

We report on the development of at-wavelength wavefront metrology for evaluation of extreme ultraviolet optics intended for use in projection lithography. Initially, a point diffraction interferometer was used and the experience acquired with this instrument led to the development of a new interferometer, the phase-shifting point diffraction interferometer. In this paper, point diffraction interferometry performed at EUV wavelengths is discussed. The design and implementation of the new phase-shifting point diffraction interferometer are described.

## Key Words

Interferometers, X-ray interferometry, Optical testing.

## Introduction

Interferometric characterization of optical aberrations is necessary to achieve near diffraction-limited imaging capability for extreme ultraviolet (EUV) projection lithography. Both at-wavelength optical system qualification and sub-nanometer wavefront measurement accuracy are needed to evaluate future multi-layer-coated EUV lithographic optics having an acceptable residual wavefront error of 0.02 waves r.m.s. or less [1]. We are developing point diffraction interferometry to meet these challenges [2, 3, 4].

Point diffraction interferometry enables direct wavefront phase measurements by detecting the interference between the unknown aberrated wavefront and a reference wave generated by diffraction from a sub-resolution pinhole. This common-path technique, applicable over a wide spectral range, can potentially achieve high absolute accuracy by utilization of a diffractive reference wavefront.

The classic point diffraction interferometer (PDI) design [5] has been used to evaluate aberrations in diffractive zone plate lenses at the wavelength of 13 nm. These initial experiments enabled the conception of the phase-shifting point diffraction interferometer (PS/PDI). This novel interferometer design overcomes the drawbacks of the conventional PDI design by providing both phase-shifting capability and significantly higher throughput.

## Experiments with the Conventional PDI

The conventional point diffraction interferometer used for EUV optics testing is illustrated in Fig. 1. The experiment utilizes narrow-band, tunable, EUV radiation from an undulator operating at the Advanced Light Source. The test optic is illuminated by a spatially coherent spherical wavefront from a pinhole source. The aberrated wavefront from the test optic is transmitted through a thin semi-transparent membrane, placed near the image plane. The reference wavefront is generated by diffraction from a sub-resolution pinhole in the mem-

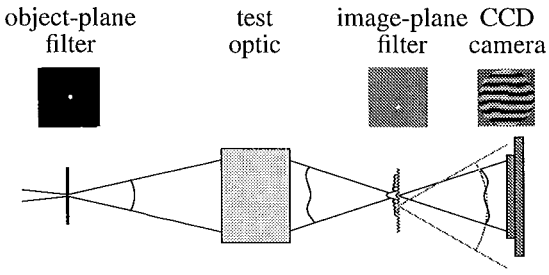


Figure 1. Conventional point diffraction interferometer.

brane. Because the pinhole samples the intensity distribution of the test wavefront to produce the reference wave, it is not possible to introduce a controlled phase shift between the test and reference waves. Without phase shifting capability, the pinhole must be placed a relatively large lateral distance from the test wave focus to produce a sufficient number of 'tilt' fringes for accurate static fringe analysis. Consequently, the amount of light transmitted through the pinhole is small and the test wave must be attenuated by three to four orders of magnitude to obtain good fringe contrast.

The PDI was used to determine aberrations in a diffractive zone plate lens at the wavelength of 13 nm. The zone plate was illuminated with a spatially-coherent, narrow-band beam from a 120-μm pinhole located 2.4 m from the 200-μm diameter zone plate. The interferometry was performed on the first diffractive order of the annular zone plate, isolated with an order sorting aperture, operated at a demagnification of 2000 and an image-side numerical aperture of about 0.08. The pinhole membrane for reference wavefront generation was placed near the focus at 1.2 mm from the zone, and the interference was recorded at 10 cm from the zone plate with an EUV CCD camera with 1024×1024 pixels and area of one square inch.

Some results of the point diffraction interferometry are summarized in Fig. 2. A series of seven recorded interferograms was analyzed with Fourier methods for static fringe pattern analysis [6, 7]. The resulting wavefront phase was fit to a set of 37 annular Zernike polynomials [8] with 30% central obscuration, matched to the zone plate aperture central stop. The average fitted wavefront aberration map, without the piston, tilt, and defocus terms, is shown in Fig. 2(a). The Zernike annular polynomial coefficients are plotted in Fig. 2(b). The indicated uncertainty of each coefficient is the standard deviation of the coefficients determined in the seven different measurements. The r.m.s. and peak-to-valley aberrations are 0.14 and 0.64 waves at 13 nm, respectively. These small measured aberrations are indicative of good imaging capabilities of the zone plate lens as well as of subnanometer resolution and precision of the interferometer.

The dominant aberration found in our measurements is 0.26 waves of astigmatism, given by annular Zernike coefficients 4 and 5. Neither the measured tilt of the zone plate with respect to the optic axis nor the estimated zone plate ellipticity of $10^{-4}$ can account for this amount of astigmatism. Some of the astigmatism may be attributed to the zone positioning fabrication errors observed in these zone plates [9]. Although zone placement errors produce mostly high spatial frequency aberrations, here their magnitude varies through two azimuthal cycles in the zone plate aperture due to sample stage drift during fabrication. This two-cycle variation can potentially contribute to low-order astigmatism. However, in addition to the astigmatism in the optic, some of the astigmatism originates from an imperfect reference wavefront, produced when the reference pinhole is too large to generate a spherical reference wavefront. Since the fringe analysis is based on the assumption of an ideal reference wavefront, reference wave aberrations contribute additively to the measured wavefront error. A 'large' pinhole placed in the outer portion of the focal pattern will sample fields that vary most rapidly along the radial direction of the focal pattern, defined by the pinhole and focal center. Consequently, an oversize pinhole will contribute to astigmatic components in the reference wave along this

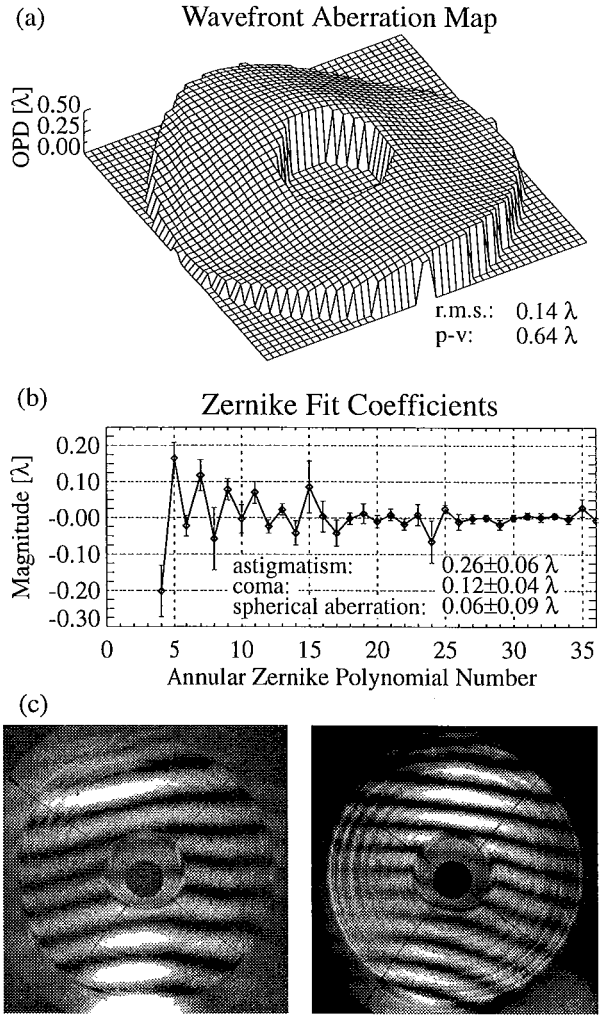


Figure 2. Aberrations of an annular zone plate lens measured at 13-nm wavelength. The average fitted wavefront optical path difference (a) and the corresponding Zernike annular polynomial coefficients (b) were determined from seven separate interferograms. Two of the measured interferograms (c).

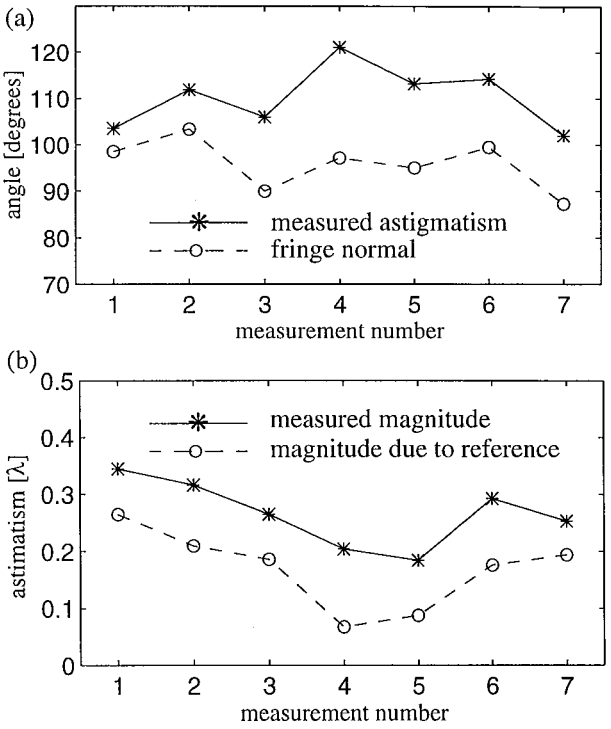


Figure 3. Correlation between the direction of the measured astigmatism and the interferogram fringe direction normal (a) in seven measurements of the same lens. The magnitude of the measured astigmatism follows the calculated astigmatism in the reference wavefront (b).

direction, orthogonal to the direction of the far-field interference tilt fringes.

For the optical system in this study, with a 30% obscured annular aperture and a numerical aperture of 0.08 at the operational wavelength of 13-nm, the diffraction-limited central focal disk diameter is 175 nm. Consequently, the reference pinhole, which must be smaller than the diffraction-limited resolution, should be below 80 nm in diameter to generate a good spherical reference wavefront [10]. These measurements were performed with an oversize ~150-nm-diameter reference pinhole because smaller pinholes were not available at the time. The measured astigmatic direction and the fringe direction normal are in fact correlated, as shown in Fig. 3(a). However, the angular offset between the two directions indicates that both the reference wave and the test optic contribute to the measured astigmatism. Assuming that in each measurement the astigmatism consists of a fixed component due to the test optic and a variable component along the fringe normal due to the reference wavefront, we have performed a non-linear least squares fit to determine these components. The magnitudes of the measured astigmatism and the calculated reference-wave astigmatism are compared in Fig. 3(b). The calculated residual astigmatism in the test optic is 0.14±0.02 waves at 13 nm, with peak at an angle of 127±3°. Although the reference wavefront astigmatism is significant here, this source of systematic error can be made negligible when a proper-size reference pinhole is used. Such pinholes, about 50 nm in diameter, are available for our future experiments [11].

## Principle of PS/PDI Operation

Although the conventional point diffraction interferometer is attractive for its compactness and relaxed temporal coherence requirements, it has practical limitations due to its low efficiency and lack of phase-shifting. The new phase-shifting point-diffraction interferometer maintains the appealing features of the PDI and provides both phase-shifting and high efficiency. In contrast to the PDI, the PS/PDI employs a low-angle beamsplitter to separate the test and reference wavefronts, as shown in Fig. 4. A coarse diffraction grating that splits an incoming beam into multiple diffraction orders is suitable for this purpose. The wavefront division produces multiple foci in the image plane of the test optic, of which two are selected with an opaque spatial filter containing a sub-resolution pinhole and a large window. One of the beams is spatially filtered with the sub-resolution pinhole to generate the diffracted reference wavefront, while the aberrated test beam passes through the window without appreciable spatial filtering. In contrast to the conventional PDI, here the test and reference wave intensities are not greatly mismatched and an attenuation of the test wavefront is not needed to obtain satisfactory fringe visibility. Since the test and reference beams must not significantly overlap in the image plane, the focal spot separation produced by the beamsplitter must be considerably larger than the lateral extent of each focal pattern.

The PS/PDI has three major advantages over the conventional PDI. First, the beam division allows control of the relative phase between the test and reference waves. For instance, a simple translation of a grating beamsplitter perpendicular to the grating lines produces a relative phase shift between any two grating orders. In addition to simplifying the fringe analysis, the phase-shifting capability removes the effects of nonuniform illumination of the optic and any fixed pattern noise, thus yielding improved measurement accuracy [12]. The second major improvement offered by the PS/PDI is its high efficiency. In the PS/PDI, the reference pinhole samples the center rather than the outer portion of the focused beam, producing an overall reference wavefront attenuation of approximately one order of magnitude rather than three to four orders of magnitude. Thus after accounting for beamsplitter losses, the amount of trans-

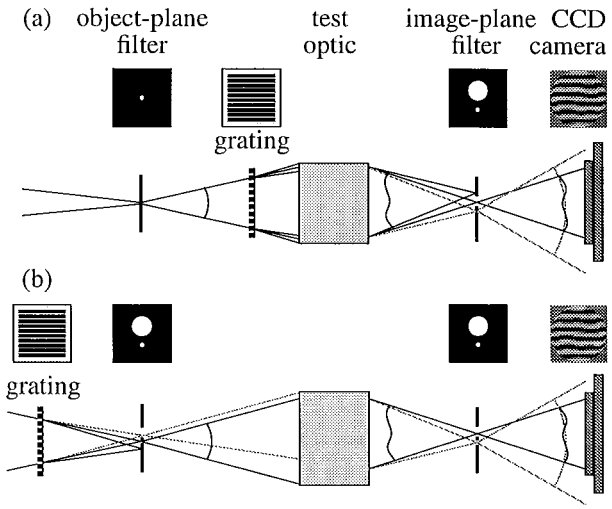


Figure 4. Two implementations of the phase-shifting point diffraction interferometer. The beamsplitter can follow the entrance pinhole spatial filter (a) or precede a two-pinhole spatial filter in the object plane (b).

mitted light is about two orders of magnitude higher in the PS/PDI design than in the conventional PDI. The third benefit is the reduction of potential reference wavefront aberrations, produced when the reference pinhole is large enough to collect a portion of the beam with significant intensity and/or phase variations. The reference pinhole illumination is more uniform when the pinhole is placed in the wide central portion of the focal pattern in the PS/PDI scheme than when it is positioned in one of the outer 'rings' in the PDI.

The beamsplitter can either be placed before the object plane, between the object plane and the optic, or between the optic and the image plane. The beam spot separation in the focal plane depends on the angular spread produced by the beamsplitter and on the position of the beamsplitter relative to the object/image plane. To obtain the necessary beam separation at focus and maintain high degree of spatial overlap inside the optical system under test and at the detector, a low-angle beamsplitter placed a large distance from the object/image plane should be used.

The effect of the beamsplitter on the measurement accuracy depends on its position relative to the object plane of the test optic. When the beamsplitter follows the object-plane spatial filter, shown in Fig. 4(a), it can potentially introduce aberrations into the measured wavefront. This is avoided when the beamsplitter precedes the object plane. To transmit both beams through the interferometer, a two-pinhole filter is then required in both the object and image planes, as illustrated in Fig. 4(b). The test beam is filtered by a sub-resolution pinhole in the object-plane mask, which removes any beamsplitter aberrations and produces spatially coherent illumination of the test optic, but is not filtered by the large window in the image-plane mask. The reference beam, passed through the large window in the object-plane mask without attenuation, is spatially filtered by the reference pinhole in the image-plane mask. This PS/PDI scheme is most useful when the illumination beam can be tightly focused to allow a low-angle beamsplitter to spatially separate the foci in the object plane. When the illumination beam is highly aberrated or originates from an extended source, the beam division must follow the entrance pinhole spatial filter.

**Practical PS/PDI Issues**

Phase-shifting point diffraction interferometry employs a beamsplitter and pinhole spatial filters to perform wavefront phase measurements. These key elements influence measurement capability in practice.

The most critical component of both the conventional PDI and the novel PS/PDI is the thin membrane that contains the reference pinhole, which must be smaller than the diffraction-limited resolution of the test optic. To accurately evaluate EUV lithographic optics with 0.1-μm resolution, pinholes with diameters around 50-75 nm are required [10]. Fabrication of such pinholes in thin membranes with electron and ion beam lithographies has progressed substantially [11, 13]. Accurate and stable alignment of the pinhole has also been demonstrated [3]. With small-size pinholes and accurate alignment as the only requirements, and the benefit of relying on diffraction to produce the reference wave, point diffraction interferometry is applicable over a wide spectral range, from the visible to the x-ray.

One limitation of point diffraction interferometry is the requirement of adequate coherent flux. This does not affect optics testing at visible or ultraviolet wavelengths, where laser sources are available. However, at EUV and x-ray wavelengths, point diffraction interferometry is most practical with high-brightness synchrotron radiation sources. The PS/PDI design, which provides throughput improvement of two orders of magnitude over the conventional PDI, can potentially be adapted to other sources.

The PS/PDI relies on the spatial separation of the test and reference waves in the image plane and is thus most useful when the test optic produces well-defined foci. The test and reference wave foci must be separated enough to prevent their overlap at the two-pinhole spatial filter, but not excessively to avoid high fringe densities. For test optics with relatively small aberrations, a reasonable separation in the focal plane is about forty times the diffraction-limited resolution, which produces

about forty far-field fringes. The size of the large test-wave transmission window in the two-pinhole filter is comparable the focal spot separation distance and limits the maximum spatial frequency measured in the test wavefront. This filtering becomes important only in measurements of relatively high spatial frequencies. For example, a transmission window, forty times the resolution in width, transmits aberrations with up to forty cycles across the aperture.

When the beamsplitter cannot precede the object plane of the test optic, as shown in Fig. 4(b), due to an aberrated or extended illumination source, the beamsplitter aberrations may contribute to systematic errors. Here we consider a simple diffraction grating beamsplitter, although other beam dividers can be used [2]. The grating substrate nonuniformities, which may introduce aberrations when the substrate is optically thick, are neglected here because the substrates are optically thin or absent in EUV transmission gratings of interest. In a simple planar diffraction grating, aberrations can arise from the non-planar illumination of the grating and from line positioning errors in the grating.

The aberrations produced by converging/diverging illumination are dominated by a third-order coma aberration, produced when the optical path to the $m^{th}$ diffractive real/virtual focus is not balanced by the tilt introduced by the grating. Higher-order coma aberrations become important above 0.1 numerical aperture. At moderate numerical apertures ($NA^2 << 1$), the peak-to-valley magnitude of the overall unbalanced coma aberration in the $m^{th}$ diffractive order is $ms NA^2$ waves, where $s$ is the separation between the foci measured in resolution units of $\lambda$/NA. For example, with 40 resolution units of focal spot separation and 0.01 numerical aperture, the peak-to-valley coma in the first diffractive order is 0.004 waves.

Errors in the grating lines can also lead to aberrations in the non-zero diffractive orders of the grating. We have determined that a grating line position error, a given fraction $q$ of the grating period in magnitude, produces a wavefront aberration in the $m^{th}$ diffractive order of $mq$ waves. The aberration profile corresponds to the grating line error profile over the illuminated portion of the grating.

It is important to note that when the substrate aberrations are negligible, the zero diffractive order is not affected by either illumination effects or grating errors. Consequently, grating aberrations do not affect the test wavefront when the zero diffractive order is chosen to be the test wavefront in the interferometer.

## Conclusions and Future Work

Point diffraction interferometry is being developed to evaluate wavefront aberrations in EUV lithographic optical systems. Measurements of diffractive zone plate lenses demonstrate the usefulness of point diffraction interferometry at EUV wavelengths. A small amount of astigmatism can be attributed to imperfections in the diffractive reference wavefront, produced by oversize reference pinholes. Proper size pinholes for generation of spherical reference wavefronts have since been fabricated.

Initial point diffraction interferometry experiments have motivated the invention of a novel interferometer, the phase-shifting point diffraction interferometer. The new design preserves the benefits of the conventional point diffraction interferometer but offers much higher throughput and improved accuracy through phase-shifting.

We are in the process of applying the phase-shifting point diffraction interferometry to testing a multilayer-coated reflective optic used in EUV projection lithography. The experiment will be performed at a new high-coherent flux beamline at the Advanced Light Source at Lawrence Berkeley National Laboratory.

## Acknowledgments

This research was supported by DARPA Defense Advanced Lithography Program, by SRC contract no. 95-MC-500, by DOE Office of Basic Energy Sciences, and by an Intel Foundation Graduate Fellowship.

## References

1. D. M. Williamson, "The elusive diffraction limit," OSA Proceedings on Extreme Ultraviolet Lithography, F. Zernike and D. T. Attwood, eds. (Optical Society of America, Washington, DC, 1995), Vol. 23, 68-76.
2. H. Medecki, E. Tejnil, K. A. Goldberg, J. Bokor, "A phase-shifting point diffraction interferometer," Opt. Lett. (in press).
3. K. A. Goldberg, R. Beguiristain, J. Bokor, H. Medecki, D. T. Attwood, K. Jackson, E. Tejnil, G. E. Sommargren, "Progress toward $\lambda$/20 EUV interferometry," J. Vac. Sci. Technol. B 13 (no. 6), 2923-7 (1995).
4. K. A. Goldberg, R. Beguiristain, J. Bokor, H. Medecki, J. Jackson, D. T. Attwood, G. E. Sommargren, J. P. Spallas, R. Hostetler, "At-wavelength testing of optics for EUV," Proc. SPIE 2437, 347-54 (1995).
5. W. P. Linnik, "A simple interferometer for the investigation of optical systems," Proceedings of the Academy of Sciences of the U. S. S. R. 1, 208 (1933).

6. M. Takeda, H. Ina, S. Kobayashi, "Fourier-transform method of fringe pattern analysis for computer-based topography and interferometry.", J. Opt. Soc. Am. 72 (no. 1), 156-60 (1982).
7. T. Kreis, "Digital holographic interference-phase measurement using the Fourier transform method," J. Opt. Soc. Am. A 3 (no. 6), 847-55 (1986).
8. V. N. Mahajan, "Zernike annular polynomials and optical aberrations of systems with annular pupils," Appl. Opt. 33 (no. 34), 8125-7 (1994).
9. E. Tejnil, K. A. Goldberg, E. H. Anderson, J. Bokor, "Zonal placement errors in zone plate lenses," these proceedings.
10. K. A. Goldberg, E. Tejnil, J. Bokor, "A 3-D numerical study of pinhole diffraction to predict the accuracy of EUV point diffraction interferometers," these proceedings.
11. E. H. Anderson, private communication.
12. D. Malacara, ed., Optical Shop Testing, second edition, (John Wiley & Sons, Inc., 1992), Ch. 14.
13. C. H. Fields, W. G. Oldham, A. K. Ray-Chaudhuri, K. D. Krenz, R. H. Stulen, "Development of an aerial image monitor for EUV lithography", these proceedings.